AMERICAN JOURNAL OF PHARMTECH RESEARCH

Journal home page: http://www.ajptr.com/

Evaluation and Optimization of *In Silico* Designed PDE_{4B} Modulators

Daniel Attard[1], Claire Shoemake[1], John Vella[1], Paweł Żmudzki[2], Grażyna Chłoń-Rzepa[2], Elżbieta Wyska[3]

1.Department of Pharmacy, Faculty of Medicine and Surgery, University of Malta, Msida
2.Department of Medicinal Chemistry, Jagiellonian University Medical College, 9 Medyczna Street, 30-688 Kraków, Poland
3.Department of Pharmacokinetics and Physical Pharmacy, Jagiellonian University Medical College, 9 Medyczna Street, 30-688 Kraków, Poland

ABSTRACT

Cyclic nucleotide phosphodiesterase 4 (PDE_4) catalyses the hydrolysis of 3',5'-cyclic AMP to 5'-AMP. Inhibition of this enzyme preserves high intracellular levels of cAMP which in turn causes suppression of TNF-α and other pro-inflammatory cytokines. It also promotes the expression of anti-inflammatory mediators. The design of small molecule inhibitors selective for PDE_{4B} subtype is considered relevant owing to the fact that this could lead to the identification of potent anti-inflammatory agents with a low side effect profile. *In vitro* evidence was indicative of the fact that a synthesized analog series of xanthine derivatives were PDE_{4B} inhibitors. This *in silico* study consequently sought to model the xanthine scaffold within the PDE_{4B} Ligand Binding Pocket (PDE_{4B}_LBP) in order to understand the critical interactions forged by this scaffold and the amino acids lining the PDE_{4B}_LBP and to use this information to model novel high affinity selective PDE_{4B} inhibitors. The results obtained from the study were structurally insightful. The xanthine scaffold was deemed suitable for the design of PDE_{4B} modulators. It was however determined that slight modifications of this scaffold could impart greater selectivity for the 4B cyclic nucleotide phosphodiesterase subtype. The modified xanthine scaffold was consequently further optimized and a series of high affinity molecules with varying physiochemical properties was identified.

Keywords: Phosphodiesterase; Xanthine derivatives; cAMP signalling; PDE_{4B} Ligand Binding Pocket; Selective inhibition**.**

*Corresponding Author Email: daniel.attard.11@um.edu.mt
Received 24 September 2016, Accepted 30 September 2016

Please cite this article as: Attard D *et al*., Evaluation and Optimization of In Silico Designed PDE4B Modulators. American Journal of PharmTech Research 2016.

INTRODUCTION

Cyclic nucleotide phosphodiesterases (PDEs) are a family of enzymes responsible for catalyzing the hydrolysis of cyclic 3',5'-AMP (cAMP) to 5'-AMP (*Figure 1*) [1,2,3]. Inhibition of the PDE_{4B} receptor results in the maintenance of high intracellular cAMP levels [4]. This suppresses Tumour Necrosis Factor-α (TNF-α) and other pro-inflammatory cytokines. It also promotes the expression of anti-inflammatory mediators, e.g. Interleukin (IL)-10. [5,6]

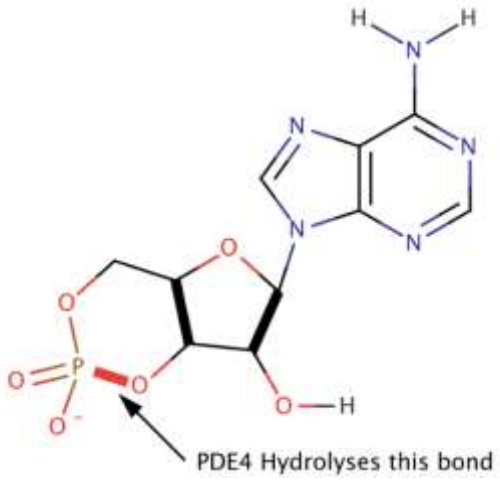

Figure 1 2D structure of cAMP, showing PDE4B action on cAMP. Produced in Marvin® Sketch v15.2.9.

PDE_4 inhibitors, through their positive effect on intracellular cAMP levels, mediate anti-inflammatory effects on almost all types of pro-inflammatory cells. In fact, the PDE_{4B} receptor subtype has been identified as a target for the management of a number of inflammatory and autoimmune diseases, including asthma, chronic obstructive pulmonary disease, inflammatory bowel disease, and psoriasis [7,8,9].

In vitro evidence from Zygmunt *et al.* [10,11] showed that an analog series of xanthine derivatives was capable of inhibiting PDE_{4B} activity This *in silico* study consequently sought to use the xanthine scaffold in order to probe the PDE_{4B}_LBP, and to understand the critical interactions that were forged between the xanthine backbone and the amino acids lining the PDE_{4B}_LBP. This scaffold was subsequently used as a lead in order to identify novel selective high-affinity inhibitors for this enzyme, on the premise that this increased selectivity would lead to a lower side effect profile. The correlation between high PDE_{4B} selectivity and low toxicity is well documented in the literature, with Jin [5,12] and Cai [13] reporting that selectivity for the PDE_{4B} receptor produced a broad spectrum of anti-inflammatory effects with decreased incidence of nausea and emesis in contrast with the non-specific inhibitor Rolipram whose intracerebral modulation of PDE_4

enzymes other than the PDE_{4B} was considered responsible for its emetic side effects [14].

MATERIALS AND METHOD

The protein databank (PDB) crystallographic deposition 4MYQ [6], describing the holo-PDE4B: antagonist A-33 complex was used as a template and verified using Procheck® [15,16] and Verify 3D® [17,18]. The small molecule was separated from the complex using Sybyl-X®v1.1 [19] and baseline binding affinity determined using Xscore® [20] v1.3.

A group of 20 xanthine derivatives obtained in the Department of Medicinal Chemistry, Faculty of Pharmacy, Jagiellonian University Medical College, Kraków, Poland was identified and used as the starting leads in the drug design process. (xanthine derivatives shown in *figure 2)*

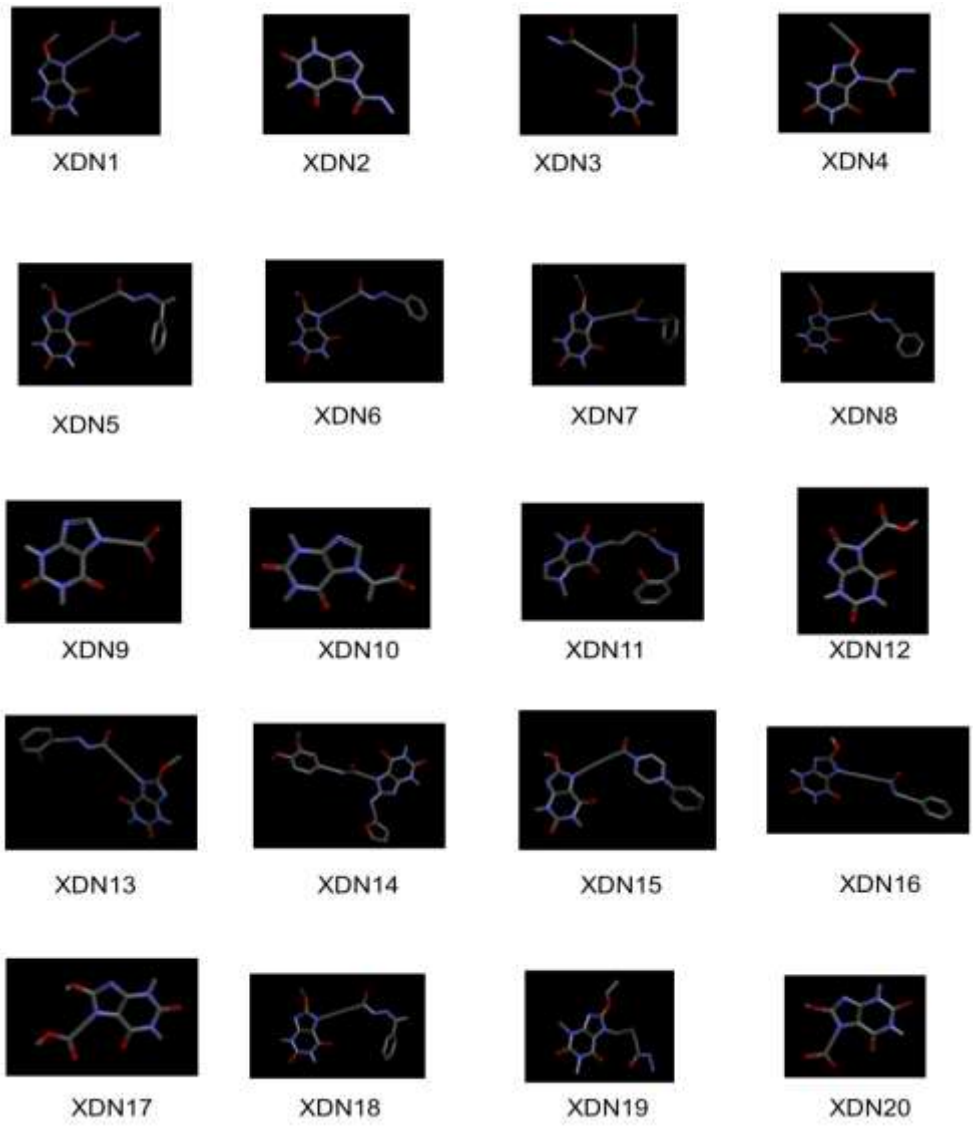

Figure 2 3D representation of all the initial xanthine derivatives generated in Sybyl-X® v1.1 (19)

Each of the 20 xanthine structures was treated similarly. Specifically, each molecule was subjected to conformational analysis in order to identify its optimal bound conformation. This process involved docking each molecule in the PDE_{4B}_LBP based on the bound co-ordinates of its cognate (A-33) small molecule inhibitor as described in the pdb crystallographic deposition 4MYQ. Each docked molecule was using Sybyl's similarity suite, allowed single bond rotation and minimisation within the PDE_{4B}_LBP. This process resulted, for each molecule, in the identification of the 20 optimal conformations within the PDE_{4B}_LBP. The Ligand Binding Affinity (LBA) (pKd) for each conformer was calculated in Xscore® [20] v1.3, while Ligand Binding Energy (LBE) ($Kcalmol^{-1}$) was calculated in Sybyl- X®v1.1 [19]. For each xanthine derivative, the LBA (pKd) and LBE ($Kcalmol^{-1}$) were plotted against conformer number (*figure 3*) and the conformer exhibiting the best combination of high LBA (pKd) and low LBE ($Kcalmol^{-1}$) was identified as optimal, on the presence that the high affinity would also be complemented by energetic stability.

In order to narrow down the optimisation process, it was decided to identify which of the 20 xanthine analogs should be further studied. 2 xanthine analogs (XDN 12 and XDN 19 in *figure 2*) were selected. The selection process involved the re-plotting, in one graph, of the LBAs (pKd) and LBEs ($Kcalmol^{-1}$) of the previously identified optimal conformations of the 20 xanthine analogs as a result of the conformational analysis process *(figure 4)*. The two conformers and therefore xanthine scaffolds having the combination of highest LBA (pKd) and low LBE ($Kcalmol^{-1}$) were promoted for further optimisation. Essentially, these selected xanthine analogs served as base scaffolds which were used for the modelling of seed fragments capable of sustaining molecular growth at user directed pre designated loci in the context of a *de novo* drug design study. Seed modelling was also guided by the identification of the crucial interactions between the selected conformations and the amino acids lining the PDE_{4B}_LBP as identified through the generation of 2D topology maps (*Figure 5*) using the software package Poseview® [21]. The moieties forging the critical interactions were consequently retained as fragment seeds with all others deemed superfluous, or less critical to affinity being computationally eliminated.

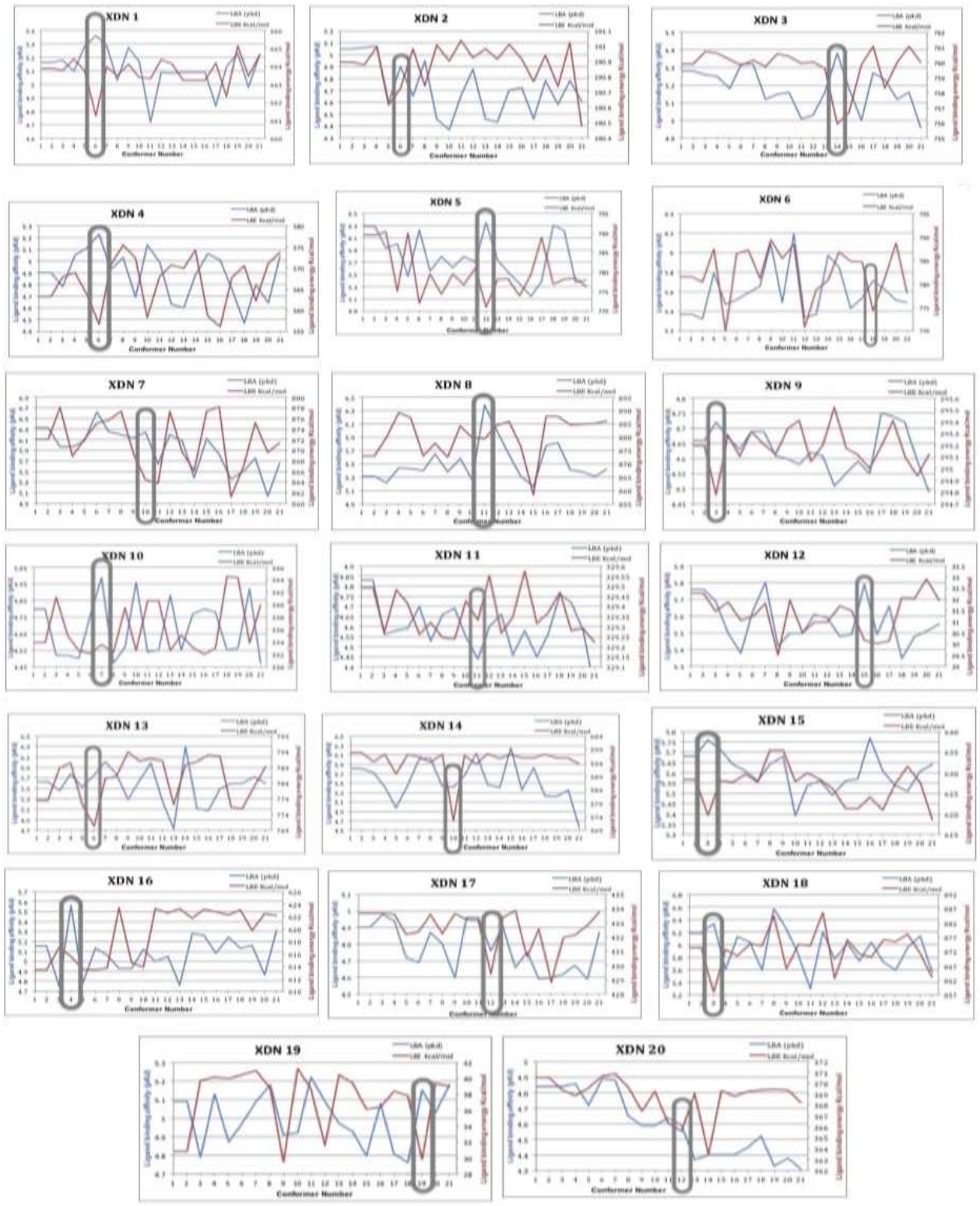

Figure 3 Graphs showing the LBA (pKd) and LBE (Kcalmol^{-1}) against conformers of all xanthine derivative. The chosen conformation for each xanthine derivative is also shown in the graph. LBA expressed as the dissociation constant (pKd) was calculated in Xscore® [20] v1.3 while LBE in Kcalmol^{-1} was calculated in Sybyl-X® [19] v1.1

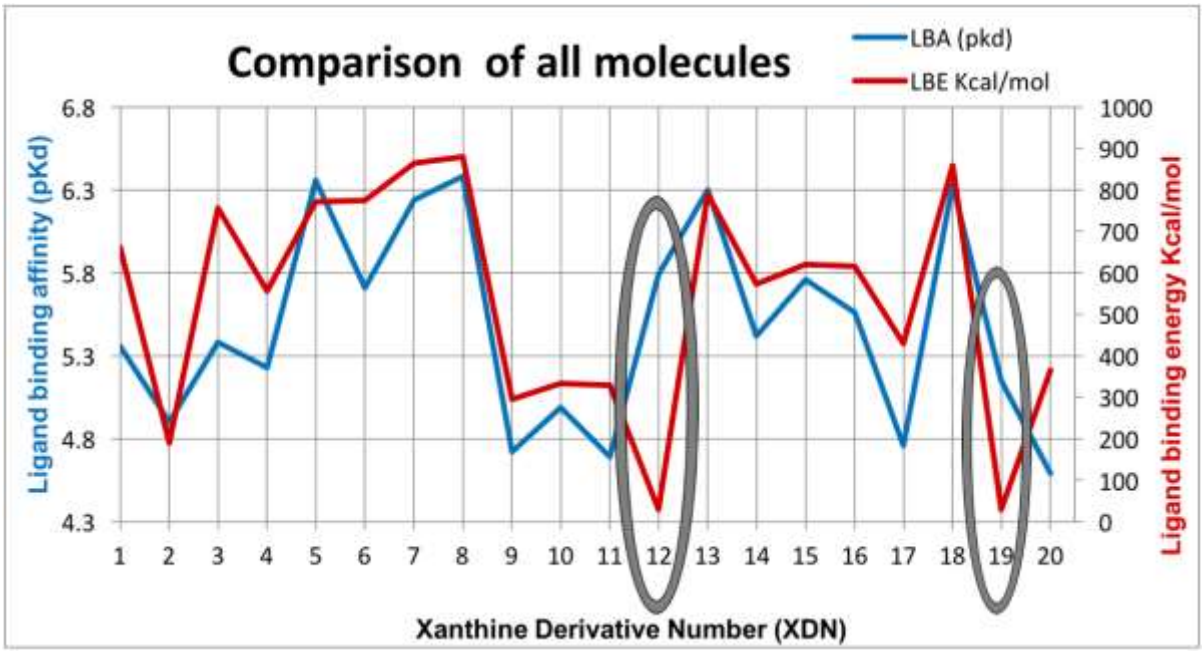

Figure 4 Comparison of LBA (pKd) and LBE (Kcalmol^{-1}) of xanthine derivative templates provided by the Jagellonian University, Poland. LBA expressed as the dissociation constant (pKd) was calculated in Xscore® [20] v1.3 while LBE in Kcalmol^{-1} was calculated in Sybyl-X® [19] v1.1.

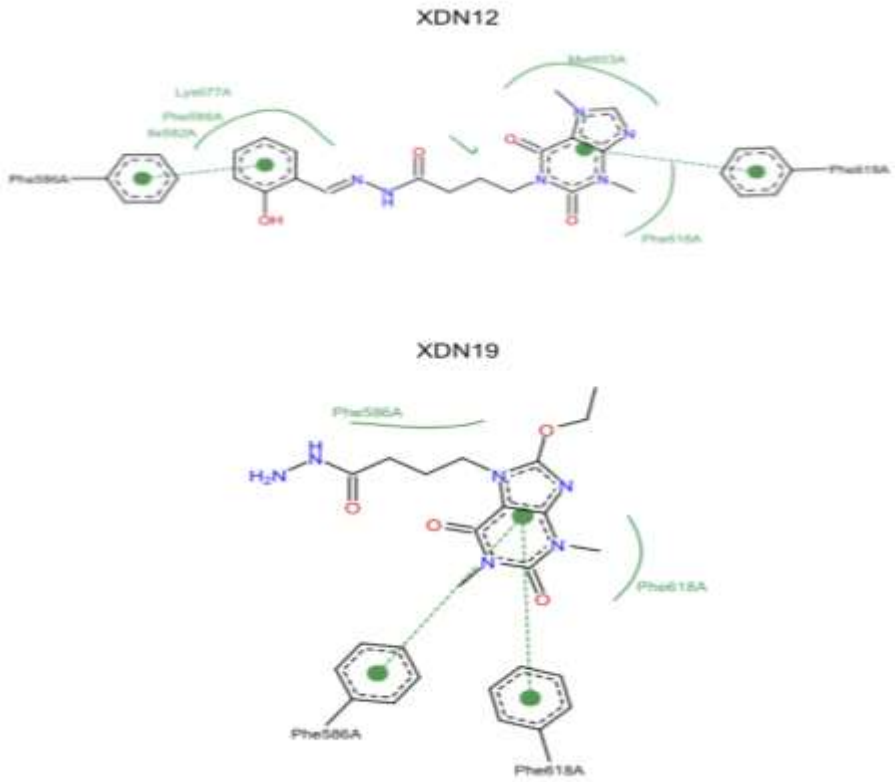

Figure 5 Poseview® [21] topology maps of XDN 12 (top) and XDN 19 (below)

De novo design was carried out in LigBuilder®v1.2 [22]. In the first part of the process, the pocket algorithm of LigBuilder®v1.2 [22] was invoked. Each of the 2 selected xanthine analogs (XDN 12 and XDN 19) in their optimal conformation as determined through conformational analysis was used to probe the PDE_{4B}_LBP. The *pocket* algorithm of LigBuilder®v1.2 [22] consequently facilitated the delineation (according to polarity) of the pharmacophoric space that the docked small molecule occupied within the PDE_{4B} receptor, and within which molecular growth could be carried out. A general pharmacophore which was designated according to polarity was also generated for each probe xanthine.

Each modelled seed structure was then planted within the 3D LBP map generated in the pocket module of LigBuilder®v1.2 [22]. The seeds were overlaid onto the analogous moiety of its xanthine parent structure in order to ensure that the optimal co-ordinates derived through conformational analysis would be present. The *GROW* algorithm of LigBuilder®v1.2 [22] was used to derive seed growth within the PDE_{4B} receptor LBPs. At the end of this process a molecular database of molecules containing structures deriving from each seed was obtained. This molecular database contained novel structures which were segregated into pharmacophorically similar families and ranked in order of decreasing LBA. Additional information about each molecule included molecular weight, logP (solubility), and a measure of synthetic feasibility. H bond donor and acceptor count was calculated for each molecule and the entire contents of each database was filtered for Lipinski rule compliance. [23].

After filtering, the optimal members of each family (based on affinity and logP) were identified and the 3 overall highest scoring molecules were subsequently submitted as query molecules to the online virtual screening database ViCi® [24] hosted by the University of Hamburg.

The submitted molecule queried the molecular database and a series of 1000 molecules were obtained in each case. The molecular cohort obtained for each query molecule was grouped into a single file which was, once again screened for Lipinski rule compliance. [23].

Sybyl-X® v1.1 [19] was used to create a protomol for each of the PDE_4 subtypes for which the pdb crystallographic depositions were available at the time of study. These were PDE_{4A}, PDE_{4B}, and PDE_{4D}. No crystallographic deposition describing the holo-PDE_{4C} was available on the pdb.

The nature of the protomol and the information that it yields from a drug design perspective warranted its creation. The protomol is identified and defined on the basis of energetically unstable amino acids situated within the core of the target enzyme, and which could potentially be stabilised through ligand binding. Typically, the protomol will extend further than the LBP such as the LBP map delineated by the pocket algorithm of LigBuilder®v1.2 [22] As it extends further, the

pharmacophoric space the protomol encloses thereby allows for a greater degree of structural innovation during the drug design process.

The molecular cohorts identified through virtual screening in ViCi® [24] and whose parent probe molecules were designed within the confines of the PDE_{4B}_LBP as delineated by the pocket algorithm of LigBuilder®v1.2 [22] were successively docked into each generated protomol (PDE_{4A}, PDE_{4B}, and PDE_{4D}). The docking process allowed molecular single bond rotations within the protomol. For each enzyme subtype, all the docked molecules were sorted and ranked by LBA (pKd). This process aided in the determination of molecular subtype specificity.

The virtual screening from the molecular database ViCi® [24], when the 3 overall highest scoring molecules from the *de novo* process were used as a query molecule after sequential docking of all the molecules into the protomols generated from PDE_{4A}, PDE_{4B} and PDE_{4D}, identified MolE (*figure 6*) as the most selective compound. *In vitro* testing of molE was carried out, with results being indicative of the requirement to further increase the aqueous solubility of this molecule. Further *in silico* manipulation of molE was consequently carried out using the software SeeSar® [25], a program that allows virtual ligand optimisation through calculation of affinity and physicochemical properties. Specifically, the PDE_{4B} protomol which was previously generated in Sybyl-X® v1.1 [19] was loaded into SeeSar® [25]. MolE was then read into the protomol and optimised within its confines through the addition of hydrophilic moieties and the substitution of hydrophobic ones at *loci* as indicated in *figure 7*. For each sequential adjustment, parameters such as affinity, logP, and torsional strength were calculated.

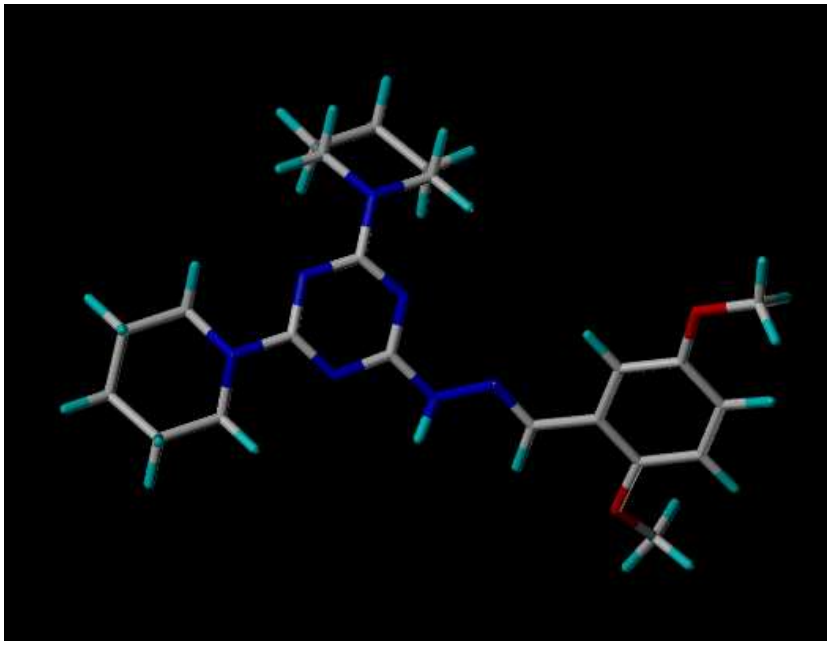

Figure 6 3D structure of molE generated in Sybyl-X® v1.1 [19]

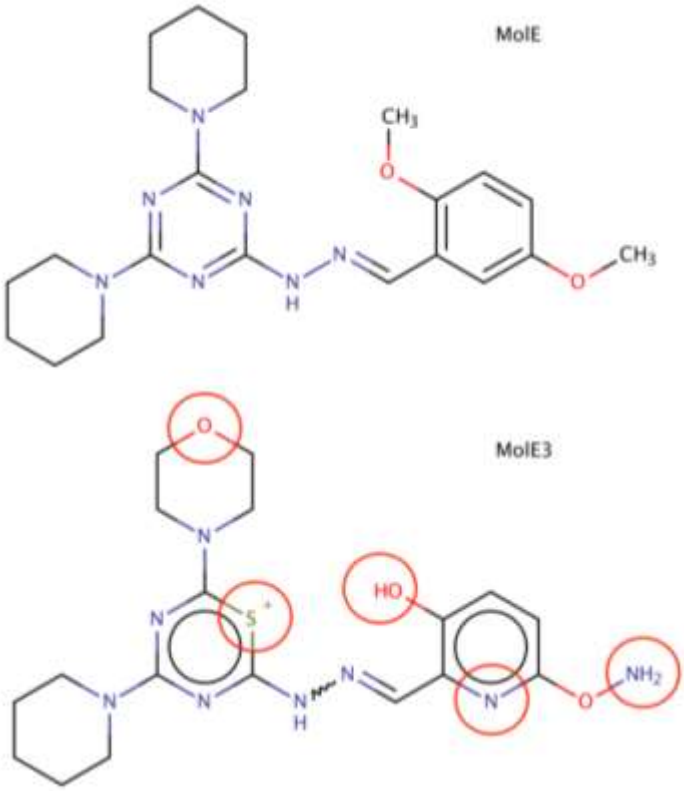

Figure 7 Molecular structure comparison of MolE3 to MolE. The red circles point out the changes carried out to optimise the water solubility of molE. 2D structure produced via Marvin® Sketch v15.2.9

RESULTS AND DISCUSSION

When the LBA (pKd) and the LBE (Kcalmol^{-1}) of the optimal conformers of each xanthine derivative (n=20) were compared, XDN 12 and 19 (*figure 3*) were deemed to exhibit the best parameter combinations. These were consequently used as scaffolds for the seed generation process. The fact that these 2 molecules adopted very distinct binding modalities within the PDE_{4B}_LBP (*figure 5)* further supported their selection.

6 seed structures *(figure 8)* were modelled for the *de novo* molecular generation process. Post molecular growth using the *pocket* algorithm of LigBuilder®v1.2 [(22)], six structurally distinct molecular families, each capable of binding to the PDE_{4B} isoenzyme with high affinity were identified. These contained a total of 1012 molecules of which, as shown in *table 1*, 240 molecules were Lipinski Rule compliant. The LBA (pKd) of these molecules ranged between 5.27 and 9.73 compared to the previously calculated baseline LBA (pKd) of the cognate PDE_{4B} inhibitor described in pdb ID 4MYQ [(6)] of 7.55. The 3 molecules FamC_H, FamD_H, FamE_H in figure 9,

were selected on the basis of their optimal LBA (pKd) to serve as query molecules for the virtual screening process.

Table 1 Affinity of the derived Lipinski compliant molecules from step 2 and the representative seed structural template for each family. Seed structures were visualized using UCSF Chimera® v1.8: http://www.cgl.ucsf.edu/chimera/download.html

Score data obtained in LigBuilder®v1.2 [22]

Family	Compliant Molecules	Affinity Range	Average Affinity	Seed Structure visualised using Chimera®
A	1	5.97	5.97	
B	42	6.96 - 5.27	6.96	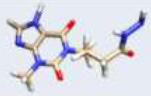
C	35	9.73 - 7.12	9.73	
D	92	9.72 - 8.31	9.72	
E	64	9.72 - 8.49	9.72	
F	6	8.26 - 7.94	8.26	
Average of highest scoring ligands :			*8.3933*	
Score of pdb cognate molecule (A-33): 7.55				

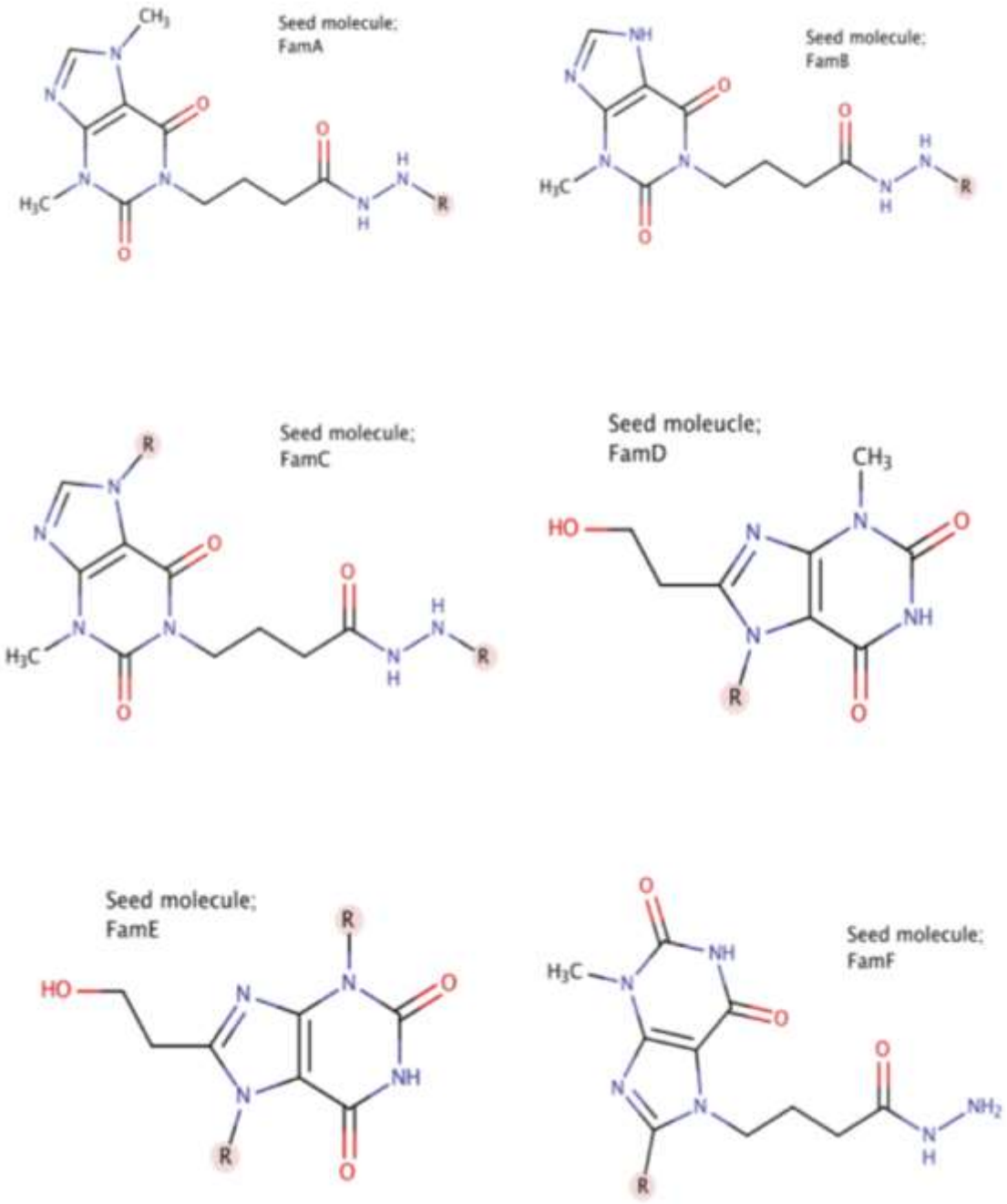

Figure 8 Seed structures created in Sybyl-X® v1.1 [(19)] and visualized using Marvin® Sketch v15.2.9. The R group denotes the designated area for molecular growth

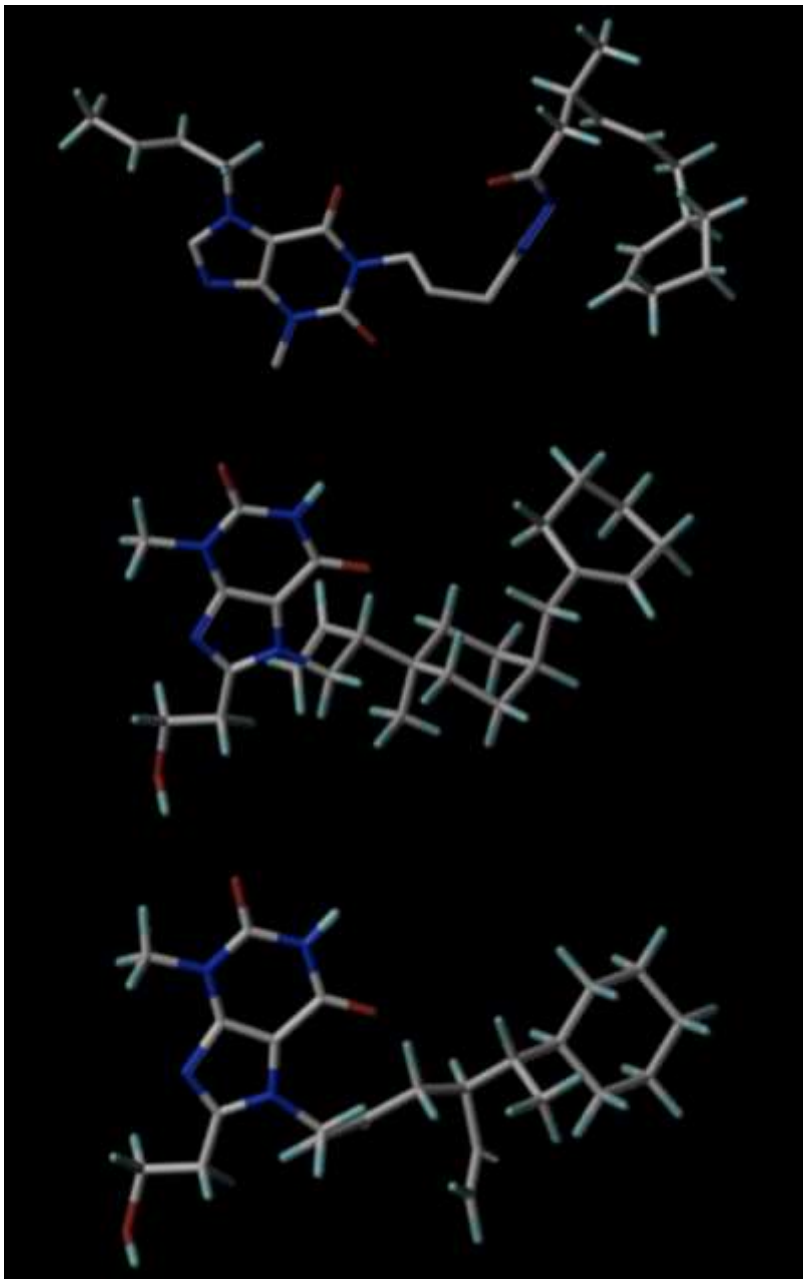

Figure 9 3D structures of selected optimal molecules from the de novo step. FamCH (top), FamDH (middle), FamEH (bottom). Visualised in Sybyl-X® v1.1 [19]

The *de novo* study as carried out was valuable in suggesting novel high-affinity binding scaffolds for the PDE_{4B} isoenzyme. Furthermore, maintenance of the moieties critical to binding and the delineation of a limited pharmacophoric space for molecular growth that was based upon the fact that it was occupied by a successful inhibitor mitigated the possibility of drastic molecular change and increased the probability of conservation of biological activity.

There are, however, also arguments to be made regarding the limitations of such an approach. Only one pdb crystallographic deposition (4MYQ [6]) was used as a template to generate a LBP and

pharmacophore. The use of consensus sampling in this case should be considered in the context of broadening further the obtained results. Furthermore, the use of a predefined LBP, even one obtained through consensus sampling, still imposes innovative limitations from a rational drug design perspective.

These limitations were mitigated in this study through the generation of three subtype specific protomols (PDE_{4A}, PDE_{4B}, and PDE_{4D}) that delineated the energetically unstable channel at the core of the protein in its entirety and which were used in order to compare the affinities of the molecules which were obtained through the virtual screening process.

Using the database ViCi® [24], the virtual screening process yielded three molecular families C, D, and, E each containing 1000 molecules, comprising 135, 133, and 186 Lipinski rule [23] compliant molecules, respectively. The optimal molecule exhibiting the best affinity and selectivity profile (as calculated after docking into each PDE subtype specific protomol) was selected from each family and a comparison was carried out as is shown in *figure 10* which compares the relative selectivity of the selected inhibitors. The affinity was expressed as a percentage increase assuming that cAMP had a baseline affinity of 0.

From the results it was shown that the percentage increase affinity of molE was 177%, this infers that molE's affinity to the PDE_{4B} is 177% greater than that of cAMP

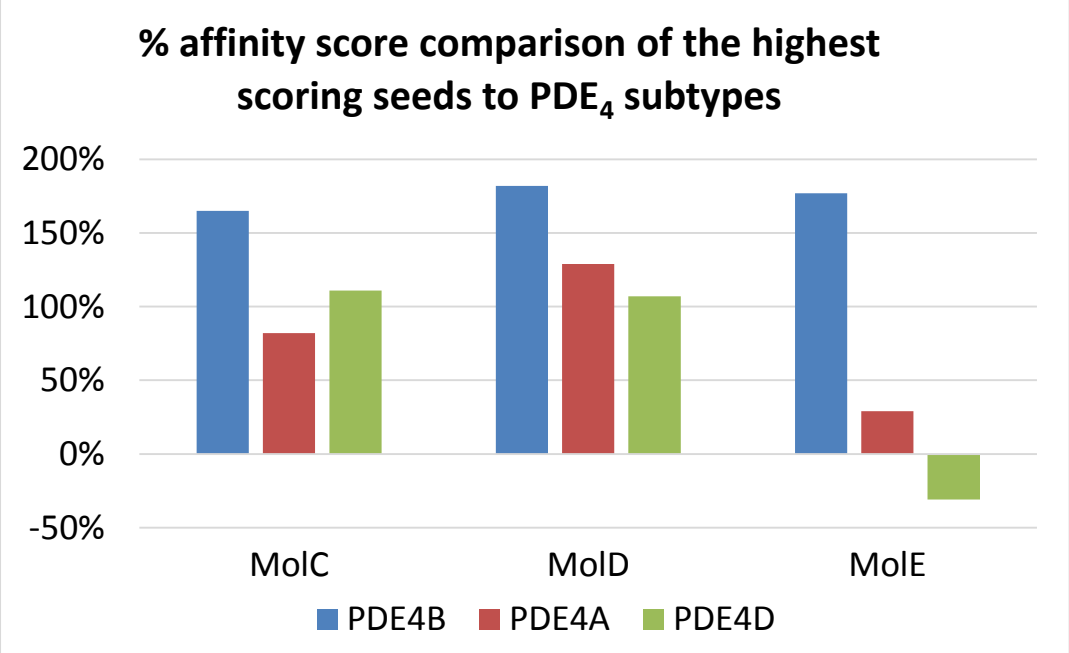

Figure 10 Comparison of percentage affinity to different PDE4 subtypes for the optimal selected ligand of each family. The percentage score was obtained by using the LBA of cAMP as a baseline.

Each family was derived through the online virtual screening program ViCi® [24]. LBA was calculated in Sybyl-X® [19] v1.1

This adjustment gives, as a percentage, the probability of a ligand to bind in comparison to the indogenous inhibitor cAMP.

Figure 10 indicates that the molecule from family E (molE) which had the highest LBA (pKd) for the target PDE_{4B} isoenzyme, also had the lowest LBA (pKd) for isoenzymes A and D. This suggests the possibility of PDE_{4B} selectivity of this compound, and this molecule will be consequently synthesised and subjected to *in vitro* testing in the future.

Given the empirically determined requirement to increase the aqueous solubility of molE, this was subjected to further *in silico* optimisation using SeeSar® [25]. This process gave rise to 7 molecules, all of which had a LBA (pKd) for the PDE_{4B} subtype that was superior, and a logP that was less than that of molE *(table 2)*. Of these, molE3 with the best selectivity profile (*figure 11)* and a low logP (l.45) was considered optimal for further studies.

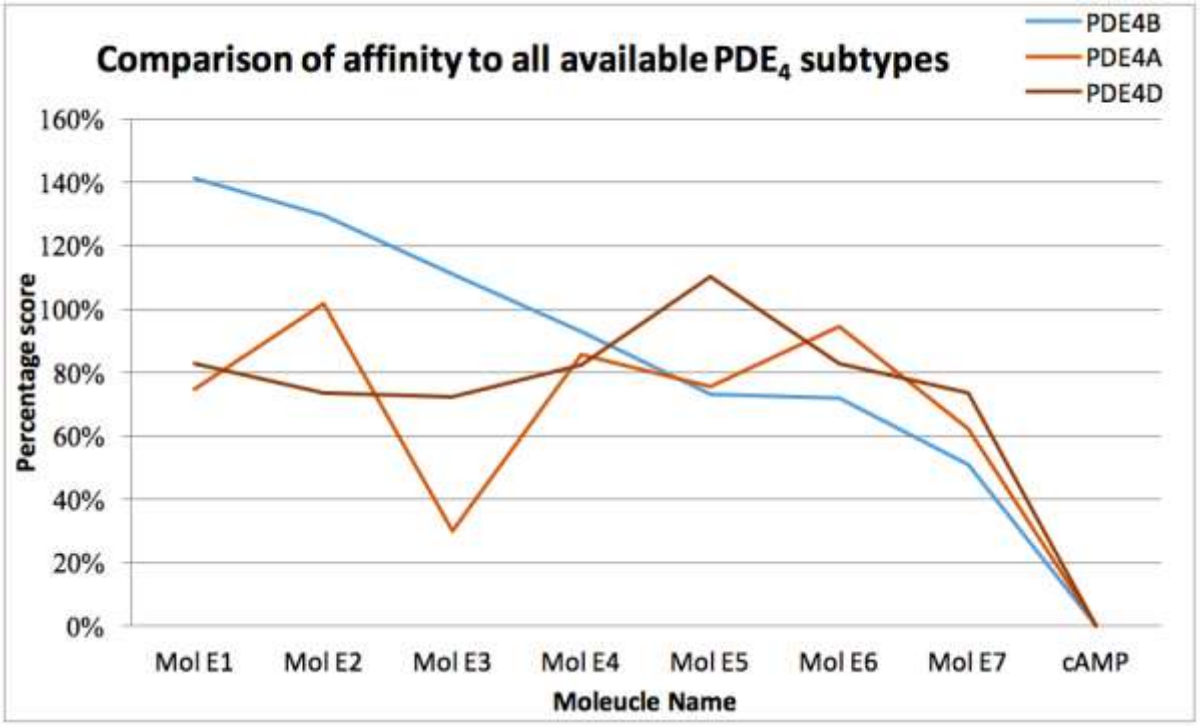

Figure 11 Comparison of percentage affinity to the different PDE_4 subtypes for the molecules derived through SeeSAR® [25]. The percentage score was obtained by using the LBA of cAMP as a baseline. LBA was calculated in Sybyl-X® [19] v1.1

Table 2:Comparison of water solubility (logP). Results were derived using SeeSAR® [25]. A low logP denotes high water solubility, whilst a high logP denotes low water solubility.

Molecule Name	logP
Mol E1	2.6
Mol E2	2.05
Mol E3	1.45
Mol E4	0.53
Mol E5	0.24
Mol E6	2.17
Mol E7	1.32
Mol E	3.32
cAMP	-0.82

The virtual screening process and subsequent optimization to molE3 represented a departure from the lead xanthine scaffold. The LBA (pKd) of these non-xanthine structures gave rise to molecules whose LBA (pKd) was just slightly higher to that of their xanthine counterparts, but whose selectivity, was predicted *in silico* to be greater, consequently implying that selectivity was increased at the expense of affinity. This is an important observation owing to the fact that increased PDE_{4B} selectivity has been correlated to a decreased adverse effect profile.

CONCLUSION

This study makes a number of important conclusions. The xanthine backbone seems to confer pan affinity across the known PDE_4 subtypes. It was only through deviation from the xanthine backbone that PDE_{4B} selectivity could be predicted *in silico*. The fact that *in vitro* testing of molE resulted in inhibition of the PDE_{4B}, validated the affinity predicted using *in silico* methods. In addition, the resulting *in vitro* inhibition showed that the predicted *in silico* affinity resulting from molE was inhibitory in nature, which confirms the direction of the study to obtain novel inhibitors. Hence, the *in vitro* result showed that molE presented as an inhibitory molecule in its interaction with the enzyme and as such, further *in silico* optimisation regarding molE would also result in ligands eliciting an inhibitory biological effect.MolE3, with a low logP, and *in silico* predicted PDE_{4B} selectivity is a new lead molecule identified through further optimisation of molE, which should be further optimized in this rational design process.

REFERENCES

1. Houslay MD, Schafer P, Zhang KY. Keynote review: phosphodiesterase-4 as a therapeutic target. Drug Discov Today. 2005 Nov; 10(22): p. 1503-1519.

2. Cai A, Hoffman CS. Determining the amino acids involved in inhibition of PDE4B by structurally-diverse compounds. Research Science Institute. 2011 Jul.
3. Hagen TJ, Mo X, Burgin AB, Fox D, Zhang Z, Gurney ME. Discovery of triazines as selective PDE4B versus PDE4D inhibitors. Bioorg Med Chem Lett. 2014; 24(16): p. 4031-4034.
4. Schett G, Victor SS, Randall MS, Schafer P. Apremilast: A Novel PDE4 Inhibitor in the Treatment of Autoimmune and Inflammatory Diseases. Ther Adv Musculoskelet Dis. 2010 Oct; 2(5): p. 271–278.
5. Jin SL, Lan L, Zoudilova M, Conti M. Specific Role of Phosphodiesterase 4B in Lipopolysaccharide-Induced Signaling in Mouse Macrophages. J Immunol. 2005; 175: p. 1523-1531.
6. Fox D, Burgin AB, Gurney ME. Structural basis for the design of selective phosphodiesterase 4B inhibitors. Cell Signal. 2014; 26(3): p. 657-663.
7. Essayan DM. Cyclic nucleotide phosphodiesterases. J Allergy Clin Immunol. 2001; 108(5): p. 671-680.
8. Page CP, Spina D. Phosphodiesterase inhibitors in the treatment of inflammatory diseases. Handb Exp Pharmacol. 2011; 204: p. 391-414.
9. Kumar N, Goldminz AM, Kim N, Gottlieb AB. Phosphodiesterase 4-targeted treatments for autoimmune diseases. BMC Medicine. 2013 May; 11(96).
10. Zygmunt M, Chłoń-Rzepa G, Sapa J. Analgesic and anti-inflammatory activity of 7-substituted purine-2,6-diones.. Pharmacol Rep. 2014; 66(6): p. 996-1002.
11. Zygmunt M, Chłoń-Rzepa G, Sapa J, Pawłowski M. Analgesic activity of new 8-methoxy-1,3-dimethyl-2,6-dioxo-purin-7-yl derivatives with carboxylic, ester or amide moieties. Pharmacol Rep. 2015; 67(1): p. 9-16.
12. Jin SL, Ding SL, Lin SL. Phosphodiesterase 4 and its inhibitors in inflammatory diseases. Chang Gung Med J. 2012; 35(3): p. 197-210.
13. Cai A. Determining the amino acids involved in inhibition of PDE4B by structurally-diverse compounds. Research Science Institute. 2011 Jun.
14. Lipworth BJ. Phosphodiesterase-4 inhibitors for asthma and chronic obstruc- tive pulmonary disease. Lancet. 2005; 365: p. 167-175.
15. Laskowski RA, MacArthur MW, Moss DS, Thornton JM. PROCHECK - a program to check the stereochemical quality of protein structures. J. App. Cryst. 1993; 26: p. 283-291

16. Laskowski RA, Rullmannn JA, MacArthur MW, Kaptein R, Thornton JM. AQUA and PROCHECK-NMR: programs for checking the quality of protein structures solved by NMR. J Biomol NMR. 1996 Dec; 8(4): p. 477-486.
17. Lüthy R, Bowie JU, Eisenberg D. Assessment of protein models with three-dimensional profiles. Nature. 1992 Mar; 356(6364): p. 83-85.
18. Bowie JU, Lüthy R, Eisenberg D. A method to identify protein sequences that fold into a known three-dimensional structure. Science. 1991 Jul; 253(5016): p. 164-170.
19. SYBYL®-X 1.1. Tripos International, 1699 South Hanley Rd., St. Louis, Missouri, 63144, USA.
20. Wang R, Lai L, Wang S. Further Development and Validation of Empirical Scoring Functions for Structure-Based Binding Affinity Prediction. J. Comput.-Aided Mol. 2002; 16: p. 11-26.
21. Stierand K, Rarey M. Drawing the PDB: Protein-Ligand Complexes in Two Dimensions. ACS Medicinal Chemistry Letters. 2010; 1(9): p. 540–54.
22. Wang R, Gao Y, Lai L. LigBuilder: A Multi-Purpose Program for Structure-Based Drug Design. J Mol Model. 2000; 6: p. 498-516.
23. Lipinski C, Lombardo F, Dominy B, Feeney P. Experimental and computational approaches to estimate solubility and permeability in drug discovery and development. Advanced Drug Delivery Reviews. 2001; 46: p. 3-26.
24. EMBL. ViCi - in-silico ligand-based drug design. [Online]. [cited 2016 2 11. Available from: http://www.embl-hamburg.de/vici/index.
25. BioSolveIT GmbH. SeeSAR. [Online].; 2016 [cited 2016 5 20. Available from: www.biosolveit.de/SeeSAR.